



# CADMIUM CHLORIDE-INDUCED SKIN ALOPECIA AND INFLAMMATION IN RATS: ANTI-INFLAMMATORY POTENTIALS OF MORINGA OLEIFERA AND MUSA SAPIENTUM VIA NF-KB/IL-4/IL-10-MEDIATED PATHWAY.

Adelaja Abdulazeez Akinlolu<sup>\*1</sup>, Gabriel Ebito<sup>2</sup>, Mubarak Ameen<sup>2</sup>, Nnaemeka Asogwa<sup>4</sup>, Kayode Odubela<sup>5</sup>, Raheem Akindele<sup>6</sup>, Bamidele Fagbohunka<sup>7</sup>, Naomi Ajayi<sup>6</sup>, Ifeoluwa Sobande<sup>6</sup> and Temitope Sikiru<sup>6</sup>.

<sup>1</sup>Department of Anatomy, Faculty of Basic Medical Sciences, Federal University of Health Sciences Otuokpo, Benue State, Nigeria.

<sup>2</sup>Department of Anatomy, Faculty of Basic Medical Sciences, Ekiti State University, Ekiti State, Nigeria.

<sup>3</sup>Department of Chemistry, Faculty of Physical Sciences, University of Ilorin, Kwara State, Nigeria.

<sup>4</sup>Central Research Laboratory, Tanke, Ilorin, Kwara State, Nigeria.

<sup>5</sup>Department of Anatomy, Faculty of Basic Medical Sciences, Olabisi Onabanjo University, Ogun State, Nigeria.

<sup>6</sup>Department of Physiology, Faculty of Basic Medical Sciences, Olabisi Onabanjo University, Ogun State, Nigeria.

<sup>7</sup>Department of Biochemistry, Faculty of Basic Medical Sciences, Olabisi Onabanjo University, Ogun State, Nigeria.

Correspondence to: Prof. Adelaja Abdulazeez Akinlolu. Email: [adelaja.akinlolu@fuhso.edu.ng](mailto:adelaja.akinlolu@fuhso.edu.ng)

## ABSTRACT

**Background:** Cadmium-induced toxicity resulted in skin carcinogenesis in rats. The mechanism underlying Cadmium-induced skin carcinogenesis remains poorly understood. Therefore, we evaluated anti-cancer potentials of *Moringa oleifera* and *Musa sapientum* in Cadmium Chloride (CdCl<sub>2</sub>)-induced skin toxicity, carcinogenesis and inflammation in rats. **Methods:** Twenty-eight adult male wistar rats (average weight of 155 g) were randomly divided into 7 groups (n = 4). Group 1 was control. Groups 2-4 and 7 received single intraperitoneal administration of 1.5 mg/Kg bodyweight of CdCl on Day 1. Thereafter, Groups 3, 4 and 7 were post-treated with 15 mg/Kg bodyweight of MO11 (oral), 15 mg/Kg bodyweight of MO11 + 7 mg/Kg bodyweight of MS06 (oral) and 3.35 mg/Kg bodyweight of Doxorubicin (*i.v.*) respectively (Days 1-17). Groups 5 and 6 received only MO11-dose and Olive Oil (vehicle) respectively (Days 1-17). Skin histopathology (Haematoxyline and Eosin technique) and ELISA concentrations of pro-inflammatory biomarkers (IL-1 $\beta$ , IL-6, IL-8 and NF-kB) and anti-inflammatory biomarkers (IL-4 and IL-10) in liver homogenates of rats of Groups 1-7 were evaluated. Computed data were statistically analysed using Mann-Whitney-U test at P  $\leq$  0.05. **Results and conclusion:** Histo-pathological evaluations showed normal skin histology in Groups 1 and 3-5, but skin histo-alterations in Groups 2 and 6. Post-treatments of CdCl<sub>2</sub>-induced skin toxicity with MO11, MO11+MS06 and Doxorubicin resulted in downregulations of IL-1 $\beta$ , IL-6, IL-8 and NF-kB, but upregulations of IL-4 and IL-10 in Groups 3, 4 and 6, compared with Group 2. Overall, MO11 and MS06 possess anticancer and anti-inflammatory potentials.

**Key words:** anti-inflammatory potentials; cadmium; *moringa oleifera*; *musa sapientum*; skin alopecia.

**DOI:** <https://dx.doi.org/10.4314/aja.v12i1.5>

## INTRODUCTION

Cadmium (Cd) is an established human and animal carcinogen (Huff et al., 2007; Wang and Du, 2013; Andjelkovic et al., 2019). Cd is one of the 10 chemicals or groups of chemicals of concern for human health according to the World Health Organization (Huff et al., 2007; Wang and Du, 2013; Andjelkovic et al., 2019). Cd is commercially used in lasers, television screens, batteries, cosmetics, paint pigments, as a barrier in nuclear fission and in galvanizing steel (Huff et al., 2007; Wang and Du, 2013; Andjelkovic et al., 2019). Cd exists as a divalent cation, which is usually complexed with other elements, such as Cadmium Chloride (CdCl<sub>2</sub>) (Huff et al., 2007; Wang and Du, 2013; Bernhoft, 2013; Andjelkovic et al., 2019). There are few experimental studies which investigated the adverse effects of Cd on the skin. Lansdown and Sampson (1996) reported that Cd-exposure (at 1.0, 0.1, and 0.01% weight/volume for 10 days) resulted in alopecia, hyperkeratosis, acanthosis, ulceration and increased mitotic index in the skin of rats and mice. In addition, exposure of surgically induced skin wounds to 1.0% CdCl<sub>2</sub> resulted in sustained oedema, epidermal hyperplasia, inflammatory cell infiltration and significant increased skin metallothionein content in rats Lansdown et al., 2001). Furthermore, Wester et al. (1992) reported human skin penetration of 12.7% (water) and 8.8 % (soil) of 5 microliters/cm<sup>2</sup> of Cd dissolved in water. Liaw et al. (2017) equally reported positive correlations between significant increase in blood Cd-content of humans and severe psoriasis following adjustment of covariates and control of confounding factors.

*Moringa oleifera* (MO) and *Musa sapientum* (MS) are established ethno-medicinal plants (Akinlolu et al., 2021). We previously isolated

MOF6, which is a sub-fraction of ethanolic extracts of MO leaves and tested its antioxidant and neuro-protective potentials. MOF6 showed significant antioxidant and neuro-protective potentials against Cuprizone-induced cerebellar damage in rats (Omotoso et al., 2018). MOF6 equally showed neuro-protective potentials against dysregulated Acetylcholinesterase concentrations in Sodium arsenite-induced neurotoxicity in rats (Akinlolu et al., 2020a). In addition, MOF6 showed hepato-protective, anti-proliferation and anti-drug resistance potentials in 7,12-Dimethylbenz(a)anthracene-induced hepatotoxicity in rats (Akinlolu et al., 2021). Furthermore, MSF1, which was fractionated from MS suckers showed hepato-protective, anti-proliferation and anti-drug resistance potentials in 7,12-Dimethylbenz(a)anthracene-induced hepatotoxicity in rats (Akinlolu et al., 2021). Despite reported Cd-induced skin carcinogenesis in animals and humans, the mechanism underlying Cd-induced skin ulceration, inflammation and carcinogenesis remains poorly understood. In addition, plants have been great sources of therapeutic drug candidates (Akinlolu et al., 2021). Therefore, in-order to understand the mechanism underlying Cd-induced skin carcinogenesis, and in-order to further identify possible plants' anticancer agents, this study evaluated anticancer effects of MO11 (isolated from *Moringa oleifera* leaves) and MS06 (isolated from *Musa sapientum* suckers) on skin gross morphology, skin histo-pathology and on biomarkers of pro-inflammation (IL-1 $\beta$ , IL-6, IL-8 and NF-kB) and anti-inflammation (IL-4 and IL-10) in CdCl<sub>2</sub>-induced skin toxicity, carcinogenesis and inflammation in adult male wistar rats.

## MATERIALS AND METHODS

### Ethical approval

Ethical approval for this study was sought and received from the Ethical Review

Committee of the University of Ilorin, Nigeria. Appropriate measures were observed to ensure minimal pain or

discomfort of rats used in this study. The ethical approval number is UERC/ASN/2018/1161. Furthermore, this research study was conducted in accordance with the internationally accepted principles for laboratory animal use and care as provided in the European Community guidelines (EEC Directive of 1986; 86/609/EEC), the Directive 2010/63/Eu of the European Parliament and of the Council of 22 September 2010 on the protection of animals used for scientific purposes and the Guidelines of the U.S. Public Health Service and NIH regarding the care and use of animals for experimentation (NIH publication #85-23, revised in 1985).

#### **Collection, authentication and deposition of MO leaves and MS suckers**

MO leaves and MS suckers were obtained locally and freshly cut from forest reserves in Ilorin, Kwara State of Nigeria. The obtained plants' samples were authenticated, deposited and assigned Herbarium Identification Numbers UILH/001/1249 and UILH/002/1182 respectively at the herbarium of the Department of Botany, University of Ilorin, Nigeria.

#### **Extraction and partitioning of fractions of MO leaves and MS suckers**

MO leaves and MS suckers were air-dried, powdered, weighed and kept in an air tight container until ready for further analyses. 4.0 Kg weight of powdered MO leaves and 5.2 kg weight of powdered MS suckers were extracted with distilled ethanol and evaporated to a dry form using a rotary evaporator. 210.2 g of MO leaves and 159.32 g of MS suckers were consequently separated into dichloromethane (DCM), ethyl acetate (EA), methanol (MeOH) and n-hexane (NH) soluble fractions in an increasing order of polarity to obtain 12 fractions (MO1 – MO12) and 8 fractions (MS01 – MS08) respectively.

#### **Column chromatography**

Column chromatography of the MO and MS fractions was executed on silica gel (70 – 230 and 240 – 300 mesh size, Merck, Germany), Merck alumina (70 – 230 mesh ASTM). Thin Layer Chromatography (TLC) was executed on pre-coated silica gel 60 F<sub>254</sub> aluminium foil (Merck, Germany) in-order to obtain pure isolates. Spots on TLC were evaluated using an ultraviolet lamp which operates at a wavelengths of 366 nm and 254 nm for fluorescence and fluorescence quenching spots respectively.

#### **Evaluations of antioxidant and antimicrobial activities of MO and MS fractions**

Antioxidant activities of plants' extracts were evaluated using modified 2,2-diphenyl-1-picrylhydrazyl method as previously described by Chaves et al., 2020. In addition, antimicrobial activities of plants' extracts were evaluated by testing the cyto-toxic potentials of each fraction against the growths of *Escherichia coli* and *Salmonella typhimurium* as previously described by Elisha et al., 2017.

#### **Purification of MO and MS fractions**

MO8, MO11 AND MS06 fractions which had the best antioxidant and antimicrobial potentials were selected and further purified on a silica gel open column, using NH, DCM, EA and MeOH in an increasing order of polarity until the most active antioxidant and anti-microbial isolates (MO11<sub>8,3</sub>, MO11<sub>8,4</sub> and MS06<sub>5</sub>) were obtained. Phytochemical screenings of MO11<sub>8,3</sub> and MO11<sub>8,4</sub> showed the presence of flavonoids, saponin, tannins, alkaloids, glycosides and steroids. The resulting grams of MO11<sub>8,3</sub> and MO11<sub>8,4</sub> were mixed together as 1.43 g of MO11, which was further tested for its anticancer and anti-inflammatory potentials in this study. Phytochemical screening of MS showed the presence of saponins, saponin glycosides, tannins, alkaloids and indole alkaloids. The resulting 1.24 g of MS06<sub>5</sub> was further tested

for its anticancer and anti-inflammatory potentials in this study as reported by Ameen and Akinlolu, 2022.

The MO isolates (MO11<sub>8,3</sub> and MO11<sub>8,4</sub>) and MS isolate (MS06<sub>5</sub>) were submitted for Liquid chromatography-mass spectrometry (LC-MS) analyses at the Chemical Purification Analysis and Screening Core --Facility, University of South Florida, Tampa, Florida, USA as reported by Ameen and Akinlolu, 2022.

### **Animal care and feeding**

24 adult male Wistar rats (average weight of 155 g and 2 months of age) were purchased from a colony breed at Badagry in Lagos state, Nigeria. The rats were randomly divided into 6 groups with 4 rats per group. The rats were acclimatized for a week at the animal house of Faculty of Pharmacy of Olabisi Onabanjo University, Nigeria before the beginning of experimental procedures. The rats were kept under standard conditions and permitted unlimited access to food and drinking water ad libitum. The bodyweights of the rats were computed on daily bases using electronic compact scale (SF-400C weighs in gram) weighing scale (Valid Enterprise, Kalbadevi, Mumbai, India).

### **Grouping of rats and extracts/drugs administration**

MO11 and MS06 were each dissolved in Olive Oil (vehicle). Rats of Control Group 1 (Baseline Control) received physiological saline only for 17 Days (Days 1-17). Each rat of Experimental Groups 2-4 and 7 received single intra-peritoneal administration of 1.5 mg/Kg bodyweight CdCl<sub>2</sub> (Sigma-Aldrich, Japan Co.) on Day 1. Rats of Group 2 (Negative Control) were left untreated throughout experimental procedure for 17 Days (Days 1-17). Thereafter, rats of Group 3 were post-treated orally with 15 mg/Kg bodyweight of MO11 for 17 Days (Days 1-17). Rats of Group 4 were post-treated orally with combined mixture of 15 mg/Kg

bodyweight of MO11 and 7 mg/Kg bodyweight of MS06 for 17 Days (Days 1-17). Rats of Group 5 received only 1 ml/Kg bodyweight of Olive Oil (vehicle) for 17 Days (Days 1-17). Rats of Group 6 were post-treated with 3.35 mg/Kg bodyweight of Doxorubicin (*i.v.*) (standard anticancer drug – Positive Control) for 17 Days (Days 1-17).

### **Completion of experimental procedures**

Twenty-four hours after the last day of administration of drugs and extracts on Day 17, the experimental procedures were completed following rats' sacrifice on Day 18. For animal sacrifice, no anesthesia were used as approved by the University Ethical Review Committee after their evaluation of the experimental protocol based on the fact that the biomarkers to be examined include enzymes and metabolic agents which may be endogenously altered by anesthetic agents requiring post-experimental control of confounding factors as previously reported by Ameen and Akinlolu, 2022.

### **Histo-pathological evaluations of the skin**

The excised normal skin portions (of Groups 1 and 3 – 6) and skin alopecia portions (of Group 2) of rats were processed for light microscopy using conventional histological procedures. Histo-pathological evaluations of the skin were conducted using Hematoxyline and Eosin technique as earlier described by Akinlolu et al., 2021. Tissue sections were photographed at the magnification of X 100.

### **Evaluations of concentrations of biomarkers in homogenates of skin of rats using Enzyme Linked Immunosorbent Assay (ELISA)**

The excised normal skin portions (of Groups 1 and 3 – 6) and skin alopecia portions (of Group 2) of rats were thoroughly homogenized using porcelain mortar and pestle in ice-cold 0.25 M sucrose. 1 g of skin

tissue was homogenized in 4 ml of 0.25 M sucrose solution. The tissue homogenates were additionally filled up to 5 ml with sucrose in a 5 ml serum bottle. Skin homogenates were consequently centrifuged at 3000 revolution per minute for 15 minutes using a centrifuge (Model 90-1). The supernatant was collected with Pasteur pipettes and placed in a freezer at -20°C, and thereafter assayed for concentrations of IL-1 $\beta$ , IL-4, IL-6, IL-8, IL-10 and NF-kB in the skin of all rats of Control Group 1 and Experimental Groups 2 – 6 using ELISA

technique as previously described by Akinlolu et al., 2021.

### **Statistical analyses**

Computed data of concentrations of each biomarker was expressed as arithmetic means  $\pm$  standard deviation. Mann-Whitney U test (Wilcoxon-Mann-Whitney Test, 2016) was used for statistical comparison of the concentration of each biomarker between two groups because the sample size of 24 is less than 30. Significant difference was confirmed at 95% confidence interval with associated P - value of less than 0.05 ( $P \leq 0.05$ ).

## **RESULTS**

### **Morphological observations of the skin**

Morphological observations showed severe skin alopecia in rats of CdCl<sub>2</sub>-only treated Group 2 (Figure 1). In contrast, no skin alopecia were noted in the skin of rats of Groups 1 and 3 – 6.

### **Histo-pathological evaluations of the skin**

Histo-pathological evaluations showed normal skin histo-architecture in rats of Groups 1 (Figure 2a) and 3-5 (Figures 2c – 2e). In contrast, histo-alterations of the stratum corneum, epidermal layer, hair follicle and sebaceous gland of the skin were observed in skin alopecia portion of rats of CdCl<sub>2</sub>-only treated Group 2 (Figure 2b). In addition, histo-pathological analyses showed mild distortion of the stratum corneum and epidermal layer of skin alopecia portion of rats of Group 6 (Figure 2f).

### **Concentrations of IL-1 $\beta$ , IL-4, IL-6, IL-8, IL-10 and NF-kB in skin homogenates of rats: CdCl<sub>2</sub>-only treated Group 2 versus Normal Saline-only Control Group 1**

Results showed statistically significant higher levels ( $P < 0.01$ ) of IL-1 $\beta$ , IL-6, IL-8 and NF-KB in rats of Group 2, when compared with Control Group 1 (Table 1 and Figures 3 - 6). In addition, results showed statistically

significant lower levels ( $P < 0.01$ ) of IL-4 and IL-10 in rats of Group 2, when compared with Control Group 1 (Table 1, Figure 7 and Figure 8).

### **Concentrations of IL-1 $\beta$ , IL-4, IL-6, IL-8, IL-10 and NF-kB in skin homogenates of rats: CdCl<sub>2</sub>-only treated Group 2 versus CdCl<sub>2</sub>-exposure + MO11 post-treated Group 3 and CdCl<sub>2</sub>-exposure + MO11 + MS06 post-treated Group 4**

Results showed statistically significant higher levels ( $P < 0.01$ ) of IL-1 $\beta$ , IL-6, IL-8 and NF-KB in rats of Group 2, when compared with Groups 3 and 4 (Table 1 and Figures 3 - 6). In addition, results showed statistically significant lower levels ( $P < 0.01$ ) of IL-4 and IL-10 in rats of Group 2, when compared with Groups 3 and 4 (Table 1, Figure 7 and Figure 8).

### **Concentrations of IL-1 $\beta$ , IL-4, IL-6, IL-8, IL-10 and NF-kB in skin homogenates of rats: CdCl<sub>2</sub>-only treated Group 2 versus CdCl<sub>2</sub>-exposure + Doxorubicin post-treated Group 6**

Results showed statistically non-significant higher levels ( $P \geq 0.05$ ) of IL-1 $\beta$  ( $P = 0.99$ ) and IL-6 ( $P = 0.16$ ) in rats of Group 2, when compared with Group 6 (Table 1, Figure 3 and Figure 4). In addition, results showed

statistically significant higher levels ( $P < 0.01$ ) of IL-8 and NF-KB in rats of Group 2, when compared with Group 6 (Table 1, Figure 5 and Figure 6). Furthermore, results showed statistically significant lower levels ( $P < 0.01$ ) of IL-4 and IL-10 in rats of Group 2, when compared with Group 6 (Table 1, Figure 7 and Figure 8).



Figure 1 : Photograph of skin alopecia in rats of CdCl<sub>2</sub>-only treated Group 2.

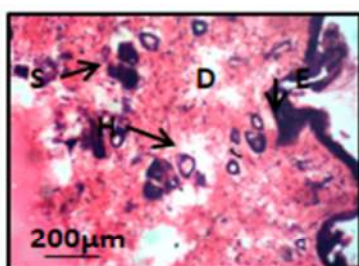


Figure 2a

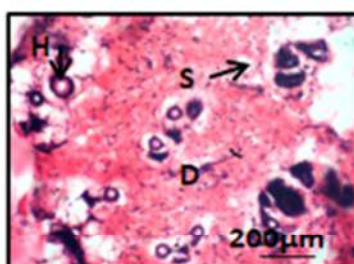


Figure 2b

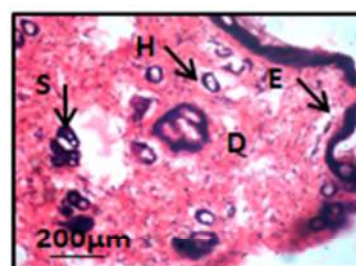


Figure 2c

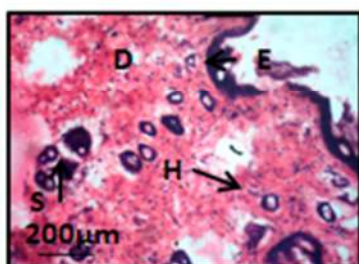


Figure 2d

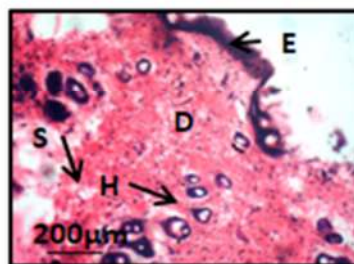


Figure 2e

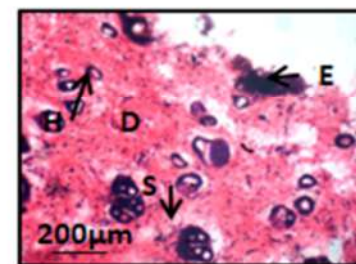


Figure 2f

**Figure 2a:** Representative photomicrograph of the Skin of rats of Group 1 which received physiological saline. Haematoxylin and Eosin. Histological analyses show normal histoarchitecture of the Skin components such as the hair follicle (H) and sebaceous gland (S). Staining intensity, cellular and morphological delineation appear normal. (S – Sebaceous gland, H – Hair follicle, D – Dermis, E - Epidermis).

**Figure 2b:** Representative photomicrograph of the Skin of rats of Group 2 which received intraperitoneal administration of 1.5 mg/Kg bodyweight of Cadmium Chloride. Haematoxylin and Eosin. Histological analyses show anomalies of the histoarchitecture of the Skin components such as the stratum corneum, epidermal layer, hair follicle (H) and sebaceous gland (S). Distortion of the stratum corneum and epidermal layer is apparent. (S – Sebaceous gland, H – Hair follicle, D – Dermis, E - Epidermis).

**Figure 2c:** Representative photomicrograph of the Skin of rats of Group 3 which received intraperitoneal administration of 1.5 mg/Kg bodyweight of Cadmium Chloride and were post-treated with 15 mg/Kg bodyweight of *Moringa oleifera*. Haematoxylin and Eosin. Histological analyses show normal histoarchitecture of the Skin components such as the hair follicle (H) and sebaceous gland (S). Staining intensity, cellular and morphological delineation appear normal. (S – Sebaceous gland, H – Hair follicle, D – Dermis, E - Epidermis).

**Figure 2d:** Representative photomicrograph of the Skin of rats of Group 4 which received intraperitoneal administration of 1.5 mg/Kg bodyweight of Cadmium Chloride and were post-treated with 15 mg/Kg bodyweight of

*Moringa oleifera* and 7mg/Kg bodyweight of *Musa sapientium* (dissolved in 1 ml of Olive oil). Haematoxylin and Eosin. Histological analyses show normal histoarchitecture of the Skin components such as the hair follicle (H) and sebaceous gland (S). Staining intensity, cellular and morphological delineation appear normal. (S – Sebaceous gland, H – Hair follicle, D – Dermis, E - Epidermis).

**Figure 2e:** Representative photomicrograph of the Skin of rats of Group 5 which received 1 ml/Kg bodyweight of Olive oil only. Haematoxylin and Eosin. Histological analyses show normal histoarchitecture of the Skin components such as the hair follicle (H) and sebaceous gland (S). Mild distortion of the epidermal layer is apparent. (S – Sebaceous gland, H – Hair follicle, D – Dermis, E - Epidermis).

**Figure 2f:** Representative photomicrograph of the Skin of rats of Group 6 which received intraperitoneal administration of 1.5 mg/Kg bodyweight of Cadmium Chloride and were post-treated with 3.35 mg/Kg bodyweight of Doxorubicin. Haematoxyline and Eosin. Histological analyses show mild anomalies of the histoarchitecture of the Skin components such as the hair follicle (H) and sebaceous gland (S). Mild distortion of the stratum corneum and epidermal layer is apparent. (S – Sebaceous gland, H – Hair follicle, D – Dermis, E - Epidermis).

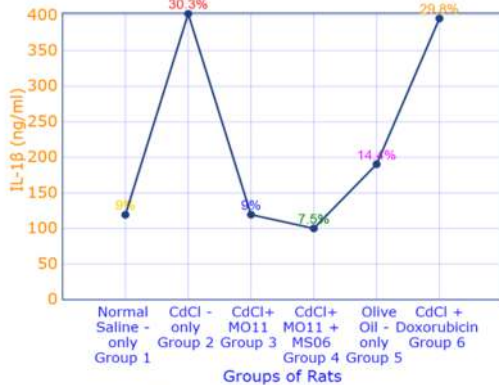


Figure 3: Concentrations of IL-1β (ng/ml) in skin homogenates of rats.

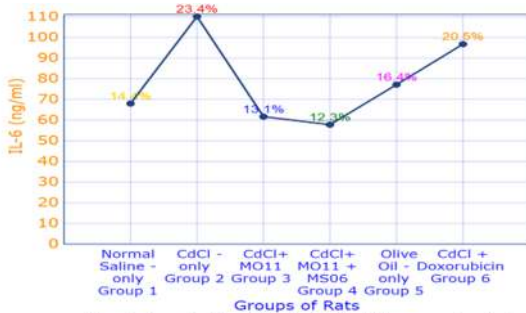


Figure 4: Concentrations of IL-6 (ng/ml) in skin homogenates of rats.

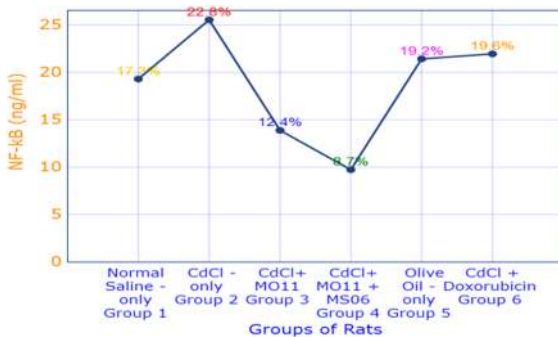


Figure 6: Concentrations of NF-kB (ng/ml) in skin homogenates of rats.

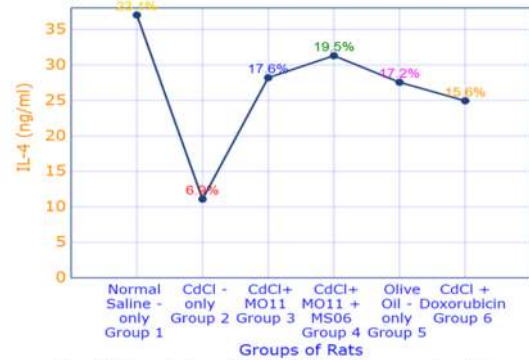


Figure 7: Concentrations of IL-4 (ng/ml) in skin homogenates of rats.

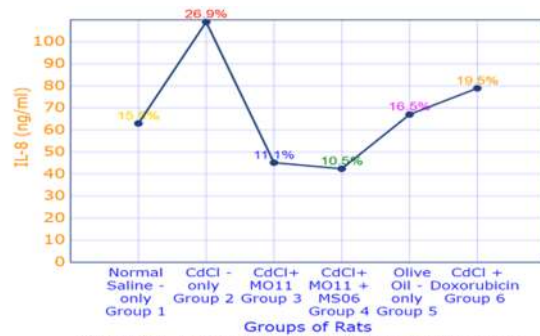


Figure 5: Concentrations of IL-8 (ng/ml) in skin homogenates of rats.

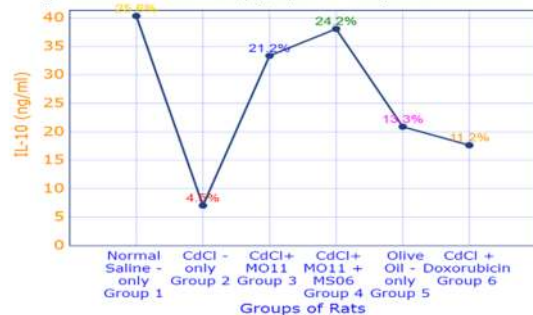


Figure 8: Concentrations of IL-10 (ng/ml) in skin homogenates of rats.

Table 1: Concentrations (ng/ml) of IL-1 $\beta$ , IL-6, IL-8, NF-kB, IL-4 and IL-10 in skin of rats.

Drug/Extract →	Normal Saline- only treated Group 1	CdCl <sub>2</sub> - only treated Group 2	CdCl <sub>2</sub> - exposure + MO11 post- treated Group 3	CdCl <sub>2</sub> - exposure + MO11 + MS06 post- treated Group 4	Olive Oil- only treated Group 5	CdCl <sub>2</sub> - exposure + Doxorubicin post-treated Group 6
IL-1 $\beta$ (ng/ml)	*119.26 <sup>c</sup> ±2.22	402.04 <sup>a</sup> ±0.56	*119.44 <sup>c</sup> ±2.78	*100.09 <sup>d</sup> ±2.38	*190.37 <sup>b</sup> ± 9.65	395.37 <sup>ab</sup> ±3.15
P - value	P < 0.01		P < 0.01	P < 0.01	P < 0.01	0.99
IL-6 (ng/ml)	*67.99 <sup>c</sup> ±0.03	110.10 <sup>a</sup> ±9.40	*61.67 <sup>d</sup> ±0.41	*57.79 <sup>e</sup> ±0.82	*77.15 <sup>b</sup> ±1.56	96.75 <sup>ab</sup> ±0.97
P - value	P < 0.01		P < 0.01	P < 0.01	P < 0.01	0.16
IL-8 (ng/ml)	*62.94 <sup>c</sup> ±1.32	108.98 <sup>a</sup> ±5.21	*45.14 <sup>d</sup> ±1.07	*42.38 <sup>d</sup> ±0.22	*67.02 <sup>b</sup> ±2.25	*78.91 <sup>ab</sup> ±3.45
P - value	P < 0.01		P < 0.01	P < 0.01	P < 0.01	P < 0.01
NF-kB (ng/ml)	*19.29 <sup>b</sup> ±0.59	25.53 <sup>a</sup> ±0.76	*13.88 <sup>c</sup> ±0.14	*9.73 <sup>d</sup> ±0.63	*21.41 <sup>ab</sup> ±0.30	*21.94 <sup>ab</sup> ±0.41
P - value	P < 0.01		P < 0.01	P < 0.01	P < 0.01	P < 0.01
IL-4 (ng/ml)	**37.05 <sup>a</sup> ±0.81	11.08 <sup>d</sup> ±0.14	**28.21 <sup>b</sup> ±0.51	**31.31 <sup>ab</sup> ±1.06	**27.56 <sup>b</sup> ±1.07	**24.95 <sup>c</sup> ±0.13
P - value	P < 0.01		P < 0.01	P < 0.01	P < 0.01	P < 0.01
IL-10 (ng/ml)	**40.33 <sup>a</sup> ±0.15	7.03 <sup>e</sup> ±1.18	**33.35 <sup>b</sup> ±0.83	**38.07 <sup>ab</sup> ±0.72	**20.88 <sup>c</sup> ±0.56	17.63 <sup>d</sup> ±1.43
P - value	P < 0.01		P < 0.01	P < 0.01	P < 0.01	P < 0.01

Mean ± SEM across the columns between groups are significantly different with a>ab>b>c>d>e. (n = 4 per group). P - value at P ≤ 0.05: Group 2 versus Groups 1 and 3 – 6 (\*\* = significant increase, \* = significant decrease).

## DISCUSSION

The observed skin alopecia (Figure 1) and histo-alterations in rats of CdCl<sub>2</sub>-only treated Group 2 (Figure 2b) confirmed Cd-induction of skin carcinogenesis, necrosis and inflammation. These observations are in agreement with those of Lansdown and Sampson, 1992 and Lansdown et al. 2001, which reported Cd-induction of skin ulceration, alopecia sustained oedema, epidermal hyperplasia and inflammatory cell infiltration in rats and mice. In addition, the findings of this study confirmed amelioration of Cd-induction of skin alopecia and histo-alteration in rats post-treated with MO11 and MS06 (Figures 2c and 2d). In contrast, post-treatments with Doxorubicin (Figure 2f) achieved lower degree of amelioration of Cd-induced skin alopecia and histo-alteration in rats.

Inflammation involves the actuation of microglia cells leading to the release of pro-

inflammatory cytokines such as IL-1 $\beta$ , IL-6, IL-8, TNF $\alpha$  and NF-kB (Shih et al., 2015; Akinlolu et al., 2020b). NF-kB upregulation results in the release and increased levels of other pro-inflammatory cytokines, hence NF-kB is opined to be the central regulator of inflammation (Shih et al., 2015). Furthermore, IL-4 and IL-10 inhibit the release of NF-kB and pro-inflammatory cytokines, and are involved in the resolution of inflammation (Shih et al., 2015).

What mechanism underlies CdCl<sub>2</sub>-induced skin inflammation associated with induced alopecia? Results of this study showed significant upregulations of IL-1 $\beta$ , IL-6, IL-8 and NF-kB, but downregulations of IL-4 and IL-10 in skin alopecia portion of rats of CdCl<sub>2</sub>-only treated Group 2, when compared with Normal saline-only treated Control Group 1 (Table 1 and Figures 3 - 8). These

observations confirm CdCl<sub>2</sub>-induction of skin inflammation, and equally indicate that CdCl<sub>2</sub>-induced inflammation possibly occurs via the NF-κB pathway. The findings of this study are in agreement with those of Ebrahimi et al. 2020, which reported Cd-induction of inflammation via upregulations of IL-1β, IL-6 and IL-8 in plasma of rats, but downregulations of IL-4 in mice.

Do MO11 and MS06 have anti-inflammatory potentials against CdCl<sub>2</sub>-induced skin inflammation? Post-treatments of CdCl<sub>2</sub>-induced skin inflammation in rats with MO11 (Group 3) and MO11 + MS06 (Group 4) resulted in significant downregulations of pro-inflammatory cytokines (IL-1β, IL-6, IL-8 and NF-κB), but significant upregulations of anti-inflammatory cytokines (IL-4 and IL-10), when compared with CdCl<sub>2</sub>-only treated Group 2 (Table 1 and Figures 3 - 8). These observations indicate that MO11 and MS06 possess anti-inflammatory potentials which were possibly mediated via the NF-κB pathway.

Are the effects of MO11 and MS06 on inflammatory biomarkers comparable with that of Doxorubicin? Post-treatments of CdCl<sub>2</sub>-induced skin inflammation in rats with Doxorubicin (Group 6) was via single-dose administration because the rats were not tolerating further administration. Hence, the possible anti-inflammatory potential of Doxorubicin in this study (Table 1 and Figures 3 - 8) instead of known pro-inflammatory potentials of Doxorubicin could have been due to inadequate administration of Doxorubicin. Therefore, the comparative potentials of MO11 and MS06 with Doxorubicin could not be ascertained in this study. The observed significant anti-inflammatory potentials of MO11 (Group 3) and MO11+MS06 (Group 4) (Table 1 and Figures 3 - 8), could have been due to the fact that MO11 and MS06 contain anticancer and anti-inflammatory compounds such as Leucine, Glutamic acid, Guanine and Phenylalanine (Ameen and Akinlolu, 2022).

## CONCLUSION

Overall, the findings of this study suggest that post-treatments with MO11 and MS06 conferred histo-protective and anti-inflammatory potentials against CdCl<sub>2</sub>-induced skin alopecia and inflammation, and resulted in downregulations of pro-inflammatory cytokines (IL-1β, IL-6, IL-8 and NF-κB), but upregulations of anti-inflammatory cytokines (IL-4 and IL-10), when compared with CdCl<sub>2</sub>-only treated Group 2. Hence, MO11 and MS06, are recommended for further evaluations as potential drug candidates for the treatments of skin alopecia and inflammation.

## ACKNOWLEDGEMENTS

The Authors acknowledge the technical support of postgraduate students of the Department of Chemistry, University of Ilorin, Nigeria during experimental procedures.

## FUNDING

No funding was received from any public or private agency.

## DATA AND MATERIALS AVAILABILITY

Original data are available upon reasonable request to the corresponding author.

## CONFLICT OF INTEREST

Authors declare no conflicts of interest.

## AUTHORS' CONTRIBUTIONS

Conception and design: AA, GE and MA(i)  
Obtaining of funding: AA, GE, MA(i), NA(i), KO, RA, BF, NA(ii), IS and TS.

Administrative, technical or logistic support: AA, GE, MA(i), NA(i), KO, RA and BF.

Collection and assembly of data: AA, GE, MA(i), NA(i), KO, RA, BF, NA(ii), IS and TS.

Critical revision of the article for intellectual content: AA, GE, MA(i), NA(i), KO, RA, BF, NA(ii), IS and TS.

Final approval of the article: AA, GE, MA(i), NA(i), KO, RA, BF, NA(ii), IS and TS.

## REFERENCES

1. Akinlolu AA, Ameen M, Quadri T, Odubela O, Omotoso G, Yahya R, et al. 2020a. Extraction, isolation and evaluation of anti-toxic principles from *Moringa oleifera* (MOF<sub>6</sub>) and *Myristica fragrans* (Trimyristin) upregulated Acetylcholinesterase concentrations in Sodium arsenite-induced neurotoxicity in rats. *J Phytomed Therapeut* 19(2):503-519.
2. Akinlolu AA, Sulaiman FA, Tajudeen S, Suleiman SK, Abdulsalam AA, Asogwa NT. 2020b. *Cajanus cajan* drives apoptosis via activation of caspase3/p53 pathway and possesses remyelination and anti-gliosis potentials in Ethidium Bromide-induced neurotoxicity in rats. *Nig J Scient Res* 19(4):286-293.
3. Akinlolu AA, Oyewopo AO, Kadir RE, Lawal A, Ademiloye J, Jubril A, et al. 2021. *Moringa oleifera* and *Musa sapientum* ameliorated 7,12-Dimethylbenz[a]anthracene-induced upregulations of Ki67 and Multidrug resistance1 genes in rats. *Int J Health Sci* 15(3):26-33.
4. Ameen AA, Akinlolu AA. 2022. Chromatography-Spectroscopic isolated MO11 (*M. oleifera*) and MS06 (*M. sapientum*) positively immunomodulated ACE2 levels in Blood, Kidney and Liver of rats. *Malaysian J Pharmaceut Sci* "in press".
5. Andjelkovic M, Buha DA, Antonijevic E, Antonijevic B, Stanic M, Kotur-Stevuljevic J, et al. 2019. Toxic effect of acute Cadmium and Lead exposure in rat blood, liver, and kidney. *Int J Evt Res Public Health* 16(2):274.
6. Bernhoft RA. 2013. Cadmium toxicity and treatment. *Scient World J ArticleID394652*:7. <http://dx.doi.org/10.1155/2013/394652>.
7. Chaves N, Antonio S, Juan CA. 2020. Quantification of the antioxidant activity of plant extracts: analysis of sensitivity and hierarchization based on the method used. *Antioxidants* 9(1):76. <https://doi.org/10.3390/antiox9010076>.
8. Dasari S, Tchounwou PB. 2014. Cisplatin in cancer therapy: molecular mechanisms of action. *European J Pharmacol* 740:364-378, 2014.
9. Dutta S, Ray S, Nagaran K. 2013. Glutamic acid as anticancer agent: An overview. *Saudi Pharmaceut J*, 21(4):337-343.
10. Ebrahimi M, Khalili N, Razi S, Keshavarz-Fathi M, Khalili N, Rezaei N. 2020. Effects of lead and cadmium on the immune system and cancer progression. *J Env Health Sci Eng* 18:335343. <https://doi.org/10.1007/s40201-020-00455-2>.
11. Elisha IL, Botha FS, McGaw LJ, Eloff JN. 2017. The antibacterial activity of extracts of nine plant species with good activity against *Escherichia coli* against five other bacteria and cytotoxicity of extracts. *BMC Complement Alt Med* 17(1):133. doi:10.1186/s12906-017-1645-z.
12. Huff J, Lunn RM, Waalkes MP, Tomatis L, Infante PF. 2007. Cadmium-induced cancers in animals and in humans. *Int J Occup Env Health* 13(2):202-12.
13. Lansdown AB, Sampson B. 1996. Dermal toxicity and percutaneous absorption of cadmium in rats and mice. *Lab Animal Sci*, 46(5):549-54.
14. Lansdown AB, King H, Aubert RE. 2001. Experimental observations in the rat on the influence of cadmium on skin wound repair. *Intern J Exp Pathol* 82(1):35-41.

15. Liaw FY, Chen WL, Kao TW, Chang YW, Huang CF. 2017. Exploring the link between cadmium and psoriasis in a nationally representative sample. *Scient Rep Article* 1723:1-7.
16. Omotoso GO, Kadir ER, Lewu SF, Gbadamosi IT, Akinlolu AA, Adunmo GO, et al. 2018. *Moringa oleifera* ameliorates cuprizone-induced cerebellar damage in adult female rats. *Res J Health Sci* 6(1):13-25.
17. Shih R-H, Wang C-Y, Yang C-M. 2015. NF-kappaB Signaling pathways in neurological inflammation: a mini review. *Front Mol Neurosci* 8:Article 77. doi:10.3389/fnmol.2015.00077.
18. Wang B, Du Y. 2013. Cadmium and its neurotoxic effects. *Oxidative Med Cellular Long* 898034. <http://doi:10.1155/2013/898034>.
19. Wester RC, Maibach HI, Sedik L, Melendres J, DiZio S, Wade M. 1992. In vitro percutaneous absorption of cadmium from water and soil into human skin. *Fundam Appl Toxicol*, 19:1-5. doi:10.1016/0272-0590(92)90021-9.